Title
WAVELENGTH MODULATION SPECTRA OF SbSI AND ITS ELECTRONIC BAND STRUCTURE

Authors
Fong, C.Y.
Petroff, Y.
Kohn, S.
et al.

Publication Date
1973-08-01

Submitted to Physical Review Letters

LBL-2225
Preprint c.1

WAVELENGTH MODULATION SPECTRA OF SbSI AND ITS ELECTRONIC BAND STRUCTURE

C. Y. Fong, Y. Petroff, S. Kohn, and Y. R. Shen

August 1973

Prepared for the U. S. Atomic Energy Commission
under Contract W-7405-ENG-48

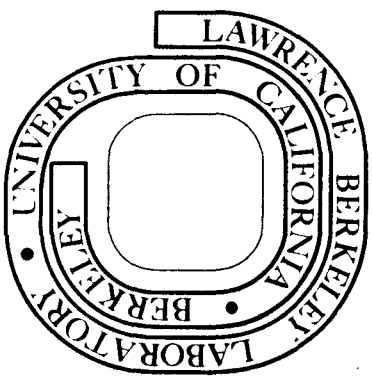

DISCLAIMER

Submitted to Physical Review Letters

LBL-2225
Preprint

UNIVERSITY OF CALIFORNIA

Lawrence Berkeley Laboratory
Berkeley, California

AEC Contract No. W-7405-eng-48

WAVELENGTH MODULATION SPECTRA OF SbSI AND ITS ELECTRONIC BAND STRUCTURE

C. Y. Fong, Y. Petroff, S. Kohn, and Y. R. Shen

AUGUST 1973

Wavelength Modulation Spectra of SbSI and Its Electronic Band Structure**

C. Y. Fong†

Department of Physics, University of California

Davis, California 95616

and

Y. Petroff,* S. Kohn and Y. R. Shen††

Department of Physics and Inorganic Materials Research Division,

Lawrence Berkeley Laboratory, University of California,

Berkeley, California 94720

Abstract

The reflectivities of SbSI and their logarithmic derivatives between 1.8 and 4.5 eV have been measured at different temperatures. The structures in the reflectivities are compared with the ones calculated independently by the empirical pseudopotential method (EPM), using the pseudopotential form factors scaled from previous band structure calculations of other crystals. The large optical anisotropy of SbSI is explained. A preliminary band structure for SbSI is presented.

The semiconducting crystal SbSI has unusual properties. a. In cooling down from room temperature, the crystal undergoes several phase transitions,[1] the high-temperature phase above 19°C being paraelectric. b. It shows very large anisotropic properties.[2] c. It has the largest known piezoelectric constant,[3] and strong nonlinear optical properties.[4] The phase transitions involve changes in crystal structure and symmetry.[1] It is then possible that

the transitions are reflected by changes in its optical spectra. In this paper, we report our experimental results on the reflectivities of SbSI and their logarithmic derivatives at different temperatures. We have found no detectable change in the optical spectra at the transitions. We then compare and identify the observed structures in the optical spectra with those obtained from an independent pseudopotential calculation for SbSI in the paraelectric phase. A preliminary band structure for SbSI is also presented. Previous calculations were done by treating SbSI as one dimensional crystal.[5]

The SbSI crystal we used had a dimension of about 10 x 1 x 1 mm^3. The $\hat{c}$-axis and the [110] direction were respectively parallel and perpendicular to the rectangular faces. Optical measurements were made on one of these faces with light polarized parallel and perpendicular to the $\hat{c}$-axis. Unfortunately, we were not able to obtain a crystal with a sufficiently large surface parallel to either $\hat{a}$ or $\hat{b}$ axis.

The apparatus for simultaneous measurements of the reflectivity and its logarithmic derivative of a sample has been described elsewhere.[6] We have measured the spectra of SbSI at many different temperatures, in particular, near the phase transitions. No detectable change in the spectra was observed at the transitions. The spectra at 5°K and 300°K are shown in Fig. 1. At low temperature, the reflectivity with $\vec{E}||\hat{c}$ has the main peaks at 2.5 and 3.08 eV and weaker ones at 2.7, 3.8, and 4.2 eV, whereas the one with $\vec{E}\perp\hat{c}$ has peaks at 2.5, 3.0, 3.37, and 3.88 eV. The corresponding derivative spectra have more fine structures as expected. The reflectivities decrease monotonically for $\hbar\omega \geq 3.5$ eV. At higher temperatures, the structures become less pronounced and shift towards lower energies. They shift by about 0.25 eV from 5 to 300°K. A particularly interesting feature of the spectra is the reflectivity with $\vec{E}||\hat{c}$ is larger than the one with $\vec{E}\perp\hat{c}$ by an overall factor of 1.6 and by a factor as

large as 2 for individual peaks.

The pseudopotential method has been described in detail elsewhere,[7] we shall mention only a few important steps pertinent to the present calculations. A. The unit cell of SbSI is orthorhombic. At room temperature, the lattice constants along the three orthogonal directions $\hat{x}(\hat{a})$, $\hat{y}(\hat{b})$ and $\hat{z}(\hat{c})$ are 8.49, 10.1 and 4.16 Å. Each unit cell contains 4 molecules in the form of a double chain, the corresponding group is D_{2h}^{16}. The positions of the atoms with respect to the center of the unit cell are expressed in units of the lattice constants:

$$\begin{aligned} \text{Sb:} \quad & \pm \begin{pmatrix} -0.375, & -0.37, & -0.25 \\ 0.118, & -0.13, & -0.25 \end{pmatrix}, \\ \text{S:} \quad & \pm \begin{pmatrix} -0.165, & -0.06, & -0.25 \\ 0.335, & 0.56, & -0.25 \end{pmatrix}, \\ \text{I:} \quad & \pm \begin{pmatrix} 0.115, & 0.325, & -0.25 \\ 0.615 & 0.175 & -0.25 \end{pmatrix}. \end{aligned} \tag{1}$$

B. The atomic form factors, $V(|\vec{G}|)$, where $\vec{G}$ is the reciprocal lattice vector, are determined as follows: a. The form factors of the S-atom, $V_S(|\vec{G}|)$, were obtained by scaling the ones from ZnS.[8] At large $|\vec{G}|$, the scaled ones were extrapolated by free hand. b. Since there is no atomic form factors of iodine, we approximated $V_I(|\vec{G}|)$ by the form factors of Cl-atom which were scaled from NaCl.[9] c. The $V_{Sb}(|\vec{G}|)$ were scaled neither from InSb nor from GaSb. Since in SbSI, the Sb atom tends to give up an electron to I-atom rather than accept electrons as in the cases of InSb and GaSb. To take into account this difference in the charge transfer, we used the $V_{Sb}(|\vec{G}|)$ scaled from the symmetric form factors of SnTe.[10] Except for the extrapolation at large $|\vec{G}|$, we did not adjust any of these form factors thus obtained. All the $V(|\vec{G}|)$'s were truncated at $|G_{max}|^2 = 14(\frac{2\pi}{\sqrt{2}c})^2$, where c is the lattice constant along the $\hat{c}$-axis. Because the ratio of the lattice constants between $\hat{y}$ and $\hat{z}$ directions is 2.42,

the corresponding $|\vec{G}_{max}|$ led to 78 pseudopotential form factors for each atom. The cutoff energies as defined in ref. 12 were $E_1 = 8.3$ and $E_2 = 20.4$. The size of the matrix was 184 x 184. Doubling the size of matrix (for ferroelectric phase) will increase the cost more than a factor of 3. There were roughly 400 plane waves contributing to the Löwdin-Brust perturbation.[13] Due to the small lattice constant along $\hat{z}$, the convergence in energies along [001] is only of the order of 0.1 eV. Since we did not adjust any of the scaled form factors, we consider the present theoretical results as preliminary.

The calculated band structure along the various symmetry lines is shown in Fig. 2. We use the notations given by Slater,[14] with, however, the ĉ-axis along $\hat{z}$. In the figure, only the 29th to 42nd bands are shown. The top of valence band corresponds to the 36th band. This band structure suggests that the fundamental gap is indirect, $\Gamma_6 \rightarrow S_1$, at 1.82 eV and the smallest direct gap occurs at Γ with an energy of 2.08 eV. At present, experimental information about the absorption edge is not sufficient to determine the nature and hence the fundamental gap energy. Harbeke[15] assigned gaps at 1.88 eV and 1.95 eV for two polarizations from his absorption measurement. However, the difference in the absorption curves can be caused by the different oscillator strengths for the two polarizations. More experiments, such as photoconductivity measurements with polarized light, are needed to pin down the band edge of SbSI.

The reflectivities, $R(\omega)$, for the two different polarizations calculated from the results of this band structure calculations with a mesh of 80 points in 1/8-th of the Brillouin zone (BZ) are given in Fig. 3. Thermal broadening and the Debye-Waller factors were not considered in the theoretical results. However, the general shapes of these reflectivities for $\hbar\omega \leq 3.0$eV resemble the measured results at 300°K (Fig. 2). For higher photon energy, the reflectivities increases. These results differ from the experimental data. Similar discrepency happens in most calculations using the empirical pseudopotential method[8]. All

these discrepencies can be attributed to the fact that the bands 29-32 and 41-42 are too close to the gap. Consequently, they contribute too much to the calculated reflectivities above 3.0eV. They also affect the calculated reflectivities below 3.0eV through the Kramer-Kronig relation. We have calculated $\varepsilon_{2\parallel}(\omega)$ and $\varepsilon_{2\perp}(\omega)$ by considering only transitions between the top 4 valence bands to the bottom 4 conduction bands. The ratio of two $\varepsilon_2(\omega)$ at 2.3eV is 1.3 and at 3.0eV is 2.5. The corresponding reflectivities are also shown in Fig. 3. Since the lattice constants at low temperature differ from the ones quoted above by 2.%[1] and no new structure in the optical data is found at the phase transition, we compare the latter reflectivities to the ones measured at 5°K. In the case of $\vec{E}||\hat{c}$, peaks in the calculated reflectivity at 2.3, 3.1 and 3.8eV agree reasonably with the experimental results. The first peak comes mainly from 36→37 transitions in the region near Γ and Λ where the dipole matrix elements for $\vec{E}||\hat{c}$ are large. The second peak is due to interband transitions 36→37, 38,39,40 and 35→37,38 in a large region with k_z, the $\hat{z}$-component of the electron momentum, about halfway between Γ and Z. The region near the XY($\hat{a}$-$\hat{b}$) plane with transitions of 33, 34→36, 37 and 38 contributes also, but the strengths of the dipole matrix elements are weaker. The important contributions to the peak at 3.8eV come from transitions of 33→38 with $0.167 \leq k_z \leq 0.333 (\frac{2\pi}{c})$. The main peak for $\vec{E} \perp \hat{c}$ is at 2.2eV and two weak structure are at 3.0 and 3.3eV. The first peak is caused by transitions of 36→37 and 38 around Y and near Σ. The regions involved in these transitions are considerably larger than the 2.3eV peak in $\vec{E}||\hat{c}$ case, however, the dipole matrix elements for these transitions are smaller and are almost constant throughout the regions. The $\hat{z}$-components of these matrix elements are mostly zero. Therefore, this peak with $\vec{E} \perp \hat{c}$ is mainly due to increase in the joint density of states. This is in contrast to the corresponding peak with $\vec{E}||\hat{c}$

where the effect of the dipole matrix elements is dominant. The joint density of states at 3.0eV in $\vec{E}\perp\hat{c}$ are the same as in $\vec{E}||\hat{c}$. Similar to the 2.2eV structure, the dipole moments are weaker in the case of $\vec{E}\perp\hat{c}$. The slightly higher reflectivity at 3.3eV compared to the structure at 3.0eV in both theory and experiment is due to additional contributions of 35→39 in the region near XY plane and 35→40 transitions near Γ. The overall ratio of the calculated reflectivities for the two polarizations in considering transitions of 4 valence bands to 4 conduction bands is about 1.4. From the above indentifications for various structure in the spectra, we therefore believe that the large optical anisotropy of SbSI is mainly due to the difference in the dipole matrix elements for the two polarizations.

Comparing the two sets of the calculated reflectivities, the ones involving less bands give the ratio 1.17 and 2.06 for two polarizations at 2.3 and 3.0eV respectively, whereas, the dashed curves in Fig. 3 give the ratio of 1.2 at 2.2eV. The peak at 3.0eV is smeared out for the reflectivity including more bands with $\vec{E}\perp\hat{c}$. The general shape of the reflectivities with transitions of 4 valence bands to 4 conduction bands for $\hbar\omega\leq 3.0$eV and the ratio at 3.0eV agree better with the experimental data. However, the magnitudes of these reflectivities are smaller than the measured ones for $\hbar\omega\leq 3.5$eV. This shows that the transitions involving other bands are important and necessary to give a better agreement between theory and experiment. Improvement on the present calculation can be achieved by adjusting the pseudopotential form factors, in particular, those of Sb. We plan to do it when the ultraviolet spectra of SbSI become available.

In conclusion, we should emphasize the preliminary nature of our calculations. The reasonable agreement between theory and experiment for $\hbar\omega \leq 3.0$eV,

obtained with no adjustment of the form factors is remarkable. This indicates that the method of scaling the atomic form factors in the calculations can be applied to very anisotropic crystals. This method is comparatively simpler than other methods for crystals with many atoms per unit cell. It is especially useful to understand the main features near the absorption edge in the optical spectra of more complex semiconductors.

** Research sponsered in part by the U.S. Atomic Energy Commission.

† Supported by the Air Force Office of Scientific Research, Air Force System Command, USAF, under Grant No. AFOSR-72-2353.

* On leave from Université de Paris, Paris VI, France.

†† Guggenheim Fellow, on leave at Laboratoire d' Optique Quantique, Orsay, France.

References

1. For example, A. Kirkuchi, Y. Oka and E. Sawaguchi, J. Phys. Soc. Japan, 23, 337 (1967).
2. For example, D. M. Bercha, V. Yu Slivka, N. N. Syrbu, I. D. Turganitsa and D. V. Chepur, Fiz. Tverd, Tela, 13, 276 (1971) (Trans. Sov. Phys. - Solid State, 13, 217 (1971)).
3. D. Berlincourt, H. Jaffe, W. Merz and R. Nitsche, Appl. Phys. Letters, 4, 61 (1964).
4. H. G. Häffle, H. Wachernig, C. Irslinger, R. Grisar and R. Nitsche, Phys. Stat. Sol. 42, 531 (1970).
5. Y. Yamada and H. Chihara, J. Phys. Soc. Japan, 21, 2085 (1966);

A. G. Khasabov and I. Ya Nikiforov, Izv. Akad. Nauk. SSR. Ser. Fiz. 34, 2480 (1970) (Trans. Bull. Acad. Sci. USSR, Phys. Ser. 34, 2204 (1970)).

6. Y. R. Shen, "Proc. of International Conf. on Moldulation Spectroscopy", Tuscon, Arizona (Nov. 23-26, 1972) (to be published in Surface Sciences); R.R.L. Zucca, Ph.D. thesis (University of California, Berkeley, 1971) (unpublished).

7. M. L. Cohen and V. Heine, Solid State Phys. 24, 37 (1970).

8. J. P. Walter and M. L. Cohen, Phys. Rev. 183, 763 (1969).

9. C. Y. Fong and M. L. Cohen, Phys. Rev. Letters 21, 22 (1968).

10. Y. W. Tung and M. L. Cohen, Phys. Rev. 180, 823 (1969).

11. E. Dönges, Z. Anorg, Chem. 263, 112 (1950); R. W. G. Wyckoff, Crystal Structure, Vol. 1, 2nd ed., Interscience, p.385 (1963).

12. M. L. Cohen and T. K. Bergstresser, Phys. Rev. 141, 789 (1966).

13. D. Brust, Phys. Rev. 134, A 1337 (1964).

14. J. C. Slater, Quantum Theory of Molecules and Solids, Vol. 2, McGraw-Hill, p. 438 (1965).

15. G. Harbeke, J. Phys. Chem. Solids 24, 957 (1963).

Figure Captions

Fig. 1 Measured reflectivities and wavelength modulated spectra of SbSI. Arrows on the curves indicate the axes of scale.

Fig. 2 Band Structure of SbSI.

Fig. 3 Comparison between the experimental and calculated reflectivities.

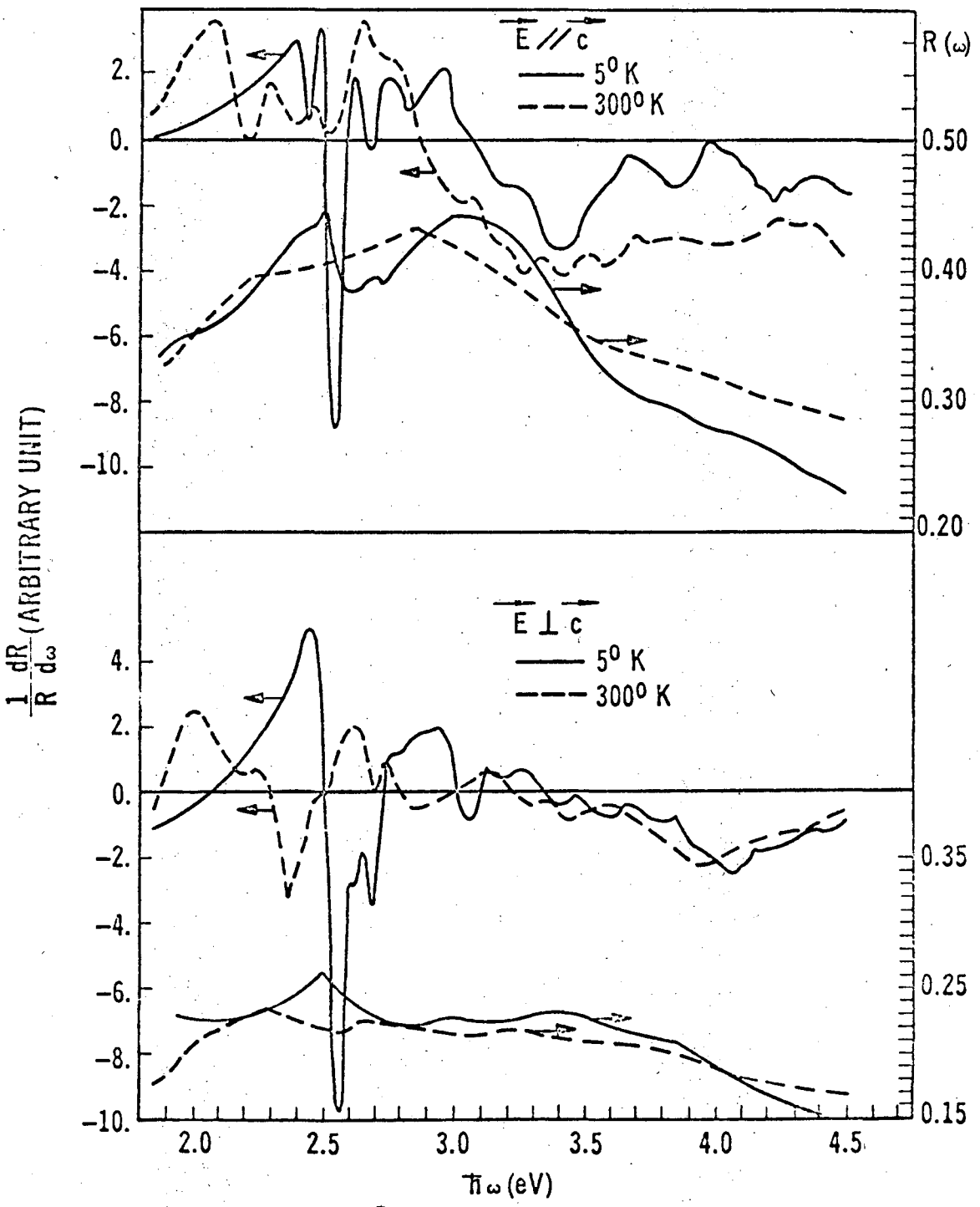
E // c
5° K
300° K
E ⊥ c
5° K
300° K
R (ω)
0.50
0.40
0.30
0.20
0.35
0.25
0.15
2.
0.
-2.
-4.
-6.
-8.
-10.
4.
2.
0.
-2.
-4.
-6.
-8.
-10.
2.0
2.5
3.0
3.5
4.0
4.5
ħω (eV)
$\frac{1}{R}\frac{dR}{d\omega}$ (ARBITRARY UNIT)

Fig. 1

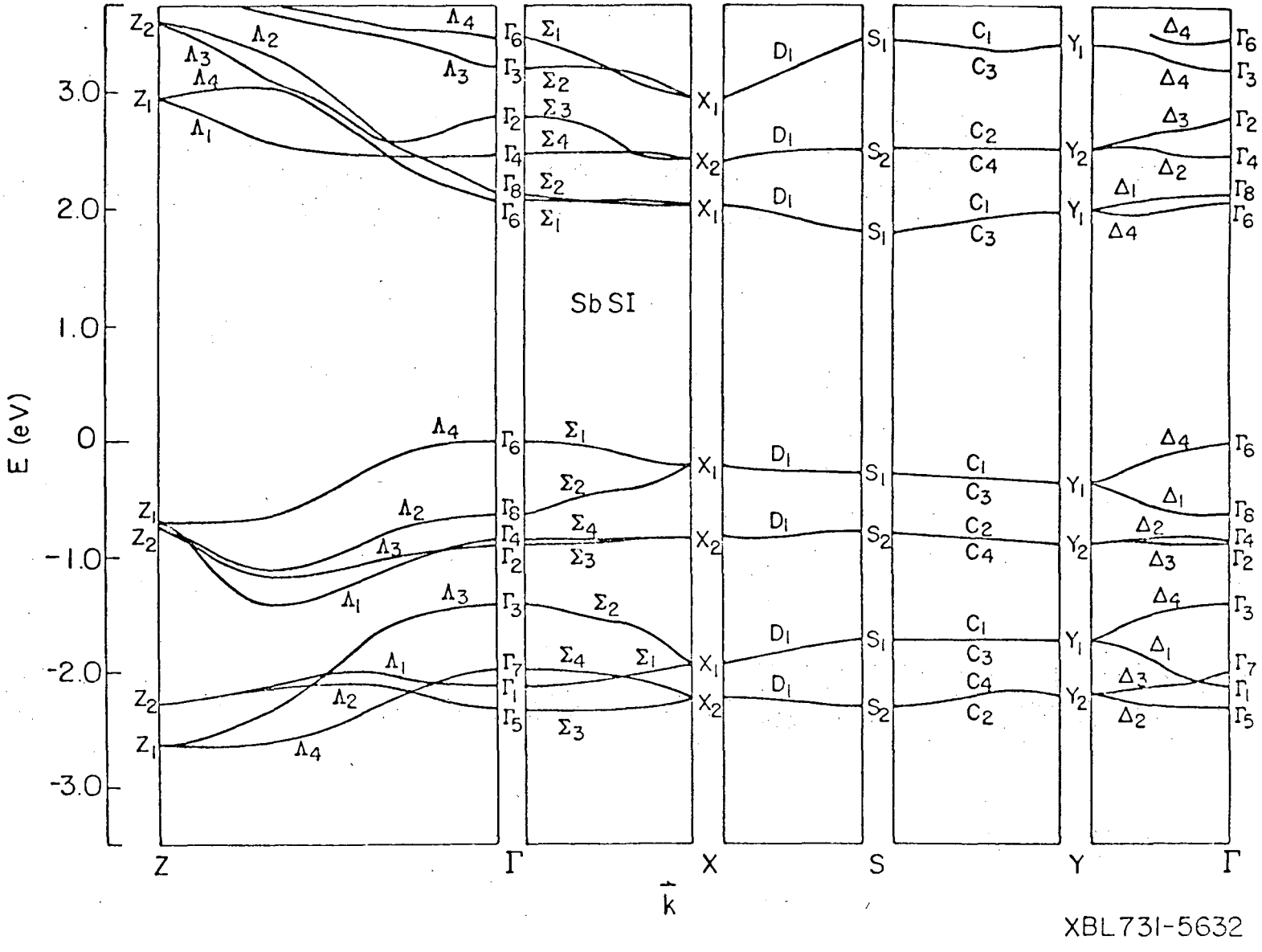

Fig. 2

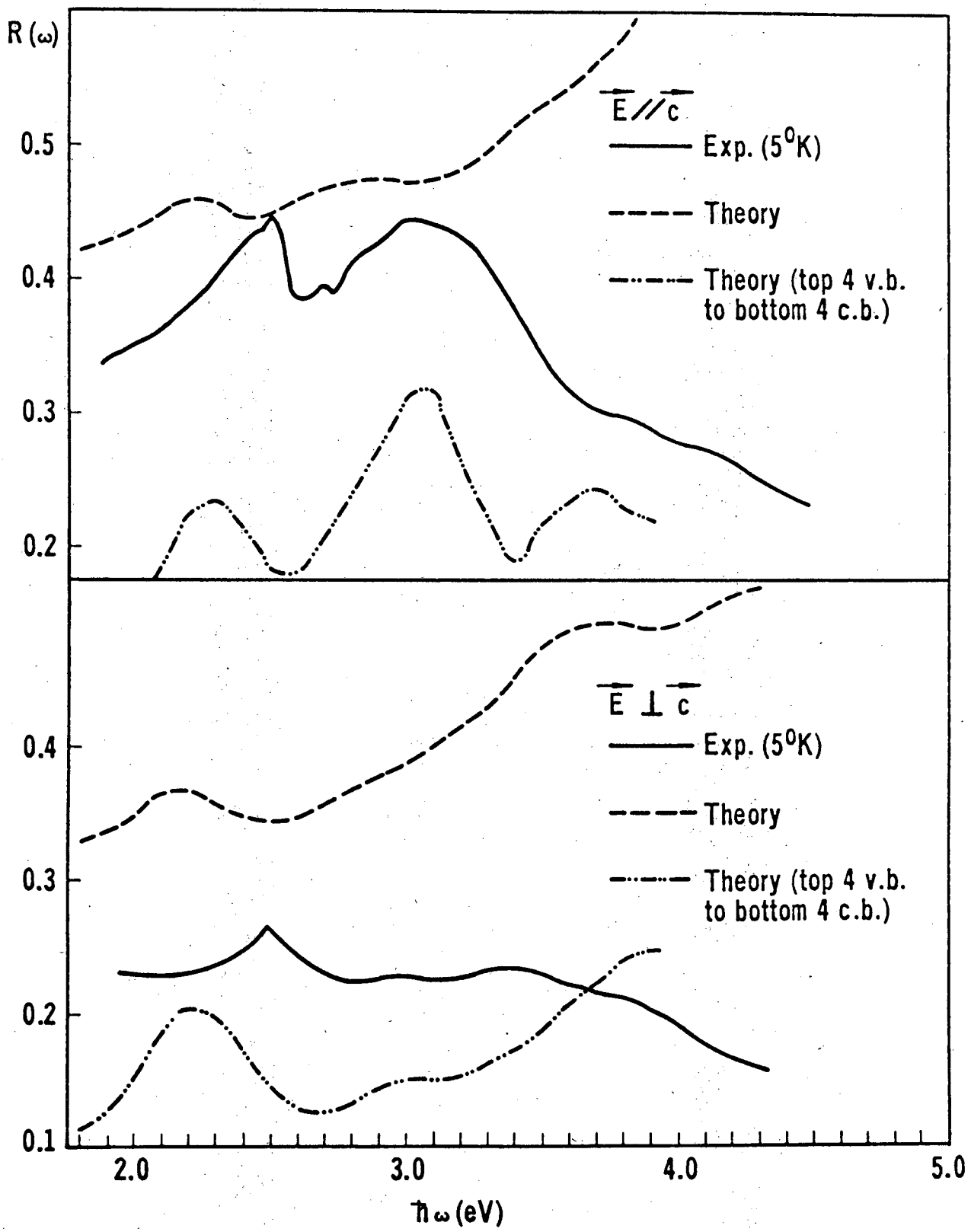
R (ω)
0.5
0.4
0.3
0.2
E // c
Exp. (5°K)
Theory
Theory (top 4 v.b. to bottom 4 c.b.)
0.4
0.3
0.2
0.1
E ⊥ c
Exp. (5°K)
Theory
Theory (top 4 v.b. to bottom 4 c.b.)
2.0
3.0
4.0
5.0
ħω (eV)

Fig. 3

Submitted to Physical Review Letters

LBL-2225
Preprint

UNIVERSITY OF CALIFORNIA

Lawrence Berkeley Laboratory
Berkeley, California

AEC Contract No. W-7405-eng-48

WAVELENGTH MODULATION SPECTRA OF SbSI AND ITS ELECTRONIC BAND STRUCTURE

C. Y. Fong, Y. Petroff, S. Kohn, and Y. R. Shen

AUGUST 1973

Wavelength Modulation Spectra of SbSI and Its Electronic Band Structure**

C. Y. Fong†

Department of Physics, University of California

Davis, California 95616

and

Y. Petroff,* S. Kohn and Y. R. Shen††

Department of Physics and Inorganic Materials Research Division,

Lawrence Berkeley Laboratory, University of California,

Berkeley, California 94720

Abstract

The reflectivities of SbSI and their logarithmic derivatives between 1.8 and 4.5 eV have been measured at different temperatures. The structures in the reflectivities are compared with the ones calculated independently by the empirical pseudopotential method (EPM), using the pseudopotential form factors scaled from previous band structure calculations of other crystals. The large optical anisotropy of SbSI is explained. A preliminary band structure for SbSI is presented.

The semiconducting crystal SbSI has unusual properties. a. In cooling down from room temperature, the crystal undergoes several phase transitions,[1] the high-temperature phase above 19°C being paraelectric. b. It shows very large anisotropic properties.[2] c. It has the largest known piezoelectric constant,[3] and strong nonlinear optical properties.[4] The phase transitions involve changes in crystal structure and symmetry.[1] It is then possible that

the transitions are reflected by changes in its optical spectra. In this paper, we report our experimental results on the reflectivities of SbSI and their logarithmic derivatives at different temperatures. We have found no detectable change in the optical spectra at the transitions. We then compare and identify the observed structures in the optical spectra with those obtained from an independent pseudopotential calculation for SbSI in the paraelectric phase. A preliminary band structure for SbSI is also presented. Previous calculations were done by treating SbSI as one dimensional crystal.[5]

The SbSI crystal we used had a dimension of about 10 x 1 x 1 mm^3. The $\hat{c}$-axis and the [110] direction were respectively parallel and perpendicular to the rectangular faces. Optical measurements were made on one of these faces with light polarized parallel and perpendicular to the $\hat{c}$-axis. Unfortunately, we were not able to obtain a crystal with a sufficiently large surface parallel to either $\hat{a}$ or $\hat{b}$ axis.

The apparatus for simultaneous measurements of the reflectivity and its logarithmic derivative of a sample has been described elsewhere.[6] We have measured the spectra of SbSI at many different temperatures, in particular, near the phase transitions. No detectable change in the spectra was observed at the transitions. The spectra at 5°K and 300°K are shown in Fig. 1. At low temperature, the reflectivity with $\vec{E}||\hat{c}$ has the main peaks at 2.5 and 3.08 eV and weaker ones at 2.7, 3.8, and 4.2 eV, whereas the one with $\vec{E}\perp\hat{c}$ has peaks at 2.5, 3.0, 3.37, and 3.88 eV. The corresponding derivative spectra have more fine structures as expected. The reflectivities decrease monotonically for $\hbar\omega \geq 3.5$ eV. At higher temperatures, the structures become less pronounced and shift towards lower energies. They shift by about 0.25 eV from 5 to 300°K. A particularly interesting feature of the spectra is the reflectivity with $\vec{E}||\hat{c}$ is larger than the one with $\vec{E}\perp\hat{c}$ by an overall factor of 1.6 and by a factor as

large as 2 for individual peaks.

The pseudopotential method has been described in detail elsewhere,[7] we shall mention only a few important steps pertinent to the present calculations. A. The unit cell of SbSI is orthorhombic. At room temperature, the lattice constants along the three orthogonal directions $\hat{x}(\hat{a})$, $\hat{y}(\hat{b})$ and $\hat{z}(\hat{c})$ are 8.49, 10.1 and 4.16 Å. Each unit cell contains 4 molecules in the form of a double chain, the corresponding group is D_{2h}^{16}. The positions of the atoms with respect to the center of the unit cell are expressed in units of the lattice constants:

$$\begin{aligned} \text{Sb}: &\quad \pm \begin{pmatrix} -0.375, & -0.37, & -0.25 \\ 0.118, & -0.13, & -0.25 \end{pmatrix}, \\ \text{S}: &\quad \pm \begin{pmatrix} -0.165, & -0.06, & -0.25 \\ 0.335, & 0.56, & -0.25 \end{pmatrix}, \\ \text{I}: &\quad \pm \begin{pmatrix} 0.115, & 0.325, & -0.25 \\ 0.615 & 0.175 & -0.25 \end{pmatrix}. \end{aligned} \tag{1}$$

B. The atomic form factors, $V(|\vec{G}|)$, where $\vec{G}$ is the reciprocal lattice vector, are determined as follows: a. The form factors of the S-atom, $V_S(|\vec{G}|)$, were obtained by scaling the ones from ZnS.[8] At large $|\vec{G}|$, the scaled ones were extrapolated by free hand. b. Since there is no atomic form factors of iodine, we approximated $V_I(|\vec{G}|)$ by the form factors of Cl-atom which were scaled from NaCl.[9] c. The $V_{Sb}(|\vec{G}|)$ were scaled neither from InSb nor from GaSb. Since in SbSI, the Sb atom tends to give up an electron to I-atom rather than accept electrons as in the cases of InSb and GaSb. To take into account this difference in the charge transfer, we used the $V_{Sb}(|\vec{G}|)$ scaled from the symmetric form factors of SnTe.[10] Except for the extrapolation at large $|\vec{G}|$, we did not adjust any of these form factors thus obtained. All the $V(|\vec{G}|)$'s were truncated at $|G_{max}|^2 = 14(\frac{2\pi}{\sqrt{2}c})^2$, where c is the lattice constant along the $\hat{c}$-axis. Because the ratio of the lattice constants between $\hat{y}$ and $\hat{z}$ directions is 2.42,

the corresponding $|\vec{G}_{max}|$ led to 78 pseudopotential form factors for each atom. The cutoff energies as defined in ref. 12 were E_1 = 8.3 and E_2 =20.4. The size of the matrix was 184 x 184. Doubling the size of matrix (for ferroelectric phase) will increase the cost more than a factor of 3. There were roughly 400 plane waves contributing to the Löwdin-Brust perturbation.[13] Due to the small lattice constant along $\hat{z}$, the convergence in energies along [001] is only of the order of 0.1 eV. Since we did not adjust any of the scaled form factors, we consider the present theoretical results as preliminary.

The calculated band structure along the various symmetry lines is shown in Fig. 2. We use the notations given by Slater,[14] with, however, the ĉ-axis along $\hat{z}$. In the figure, only the 29th to 42nd bands are shown. The top of valence band corresponds to the 36th band. This band structure suggests that the fundamental gap is indirect, $\Gamma_6 \rightarrow S_1$, at 1.82 eV and the smallest direct gap occurs at Γ with an energy of 2.08 eV. At present, experimental information about the absorption edge is not sufficient to determine the nature and hence the fundamental gap energy. Harbeke[15] assigned gaps at 1.88 eV and 1.95 eV for two polarizations from his absorption measurement. However, the difference in the absorption curves can be caused by the different oscillator strengths for the two polarizations. More experiments, such as photoconductivity measurements with polarized light, are needed to pin down the band edge of SbSI.

The reflectivities, $R(\omega)$, for the two different polarizations calculated from the results of this band structure calculations with a mesh of 80 points in 1/8-th of the Brillouin zone (BZ) are given in Fig. 3. Thermal broadening and the Debye-Waller factors were not considered in the theoretical results. However, the general shapes of these reflectivities for $\hbar\omega \leq 3.0$eV resemble the measured results at 300°K (Fig. 2). For higher photon energy, the reflectivities increases. These results differ from the experimental data. Similar discrepency happens in most calculations using the empirical pseudopotential method[8]. All

these discrepencies can be attributed to the fact that the bands 29-32 and 41-42 are too close to the gap. Consequently, they contribute too much to the calculated reflectivities above 3.0eV. They also affect the calculated reflectivities below 3.0eV through the Kramer-Kronig relation. We have calculated $\varepsilon_{2\parallel}(\omega)$ and $\varepsilon_{2\perp}(\omega)$ by considering only transitions between the top 4 valence bands to the bottom 4 conduction bands. The ratio of two $\varepsilon_2(\omega)$ at 2.3eV is 1.3 and at 3.0eV is 2.5. The corresponding reflectivities are also shown in Fig. 3. Since the lattice constants at low temperature differ from the ones quoted above by 2.%[1] and no new structure in the optical data is found at the phase transition, we compare the latter reflectivities to the ones measured at 5°K. In the case of $\vec{E}||\hat{c}$, peaks in the calculated reflectivity at 2.3, 3.1 and 3.8eV agree reasonably with the experimental results. The first peak comes mainly from 36→37 transitions in the region near Γ and Λ where the dipole matrix elements for $\vec{E}||\hat{c}$ are large. The second peak is due to interband transitions 36→37, 38,39,40 and 35→37,38 in a large region with k_z, the $\hat{z}$-component of the electron momentum, about halfway between Γ and Z. The region near the XY($\hat{a}$-$\hat{b}$) plane with transitions of 33, 34→36, 37 and 38 contributes also, but the strengths of the dipole matrix elements are weaker. The important contributions to the peak at 3.8eV come from transitions of 33→38 with $0.167 \leq k_z \leq 0.333(\frac{2\pi}{c})$. The main peak for $\vec{E} \perp \hat{c}$ is at 2.2eV and two weak structure are at 3.0 and 3.3eV. The first peak is caused by transitions of 36→37 and 38 around Y and near Σ. The regions involved in these transitions are considerably larger than the 2.3eV peak in $\vec{E}||\hat{c}$ case, however, the dipole matrix elements for these transitions are smaller and are almost constant throughout the regions. The $\hat{z}$-components of these matrix elements are mostly zero. Therefore, this peak with $\vec{E} \perp \hat{c}$ is mainly due to increase in the joint density of states. This is in contrast to the corresponding peak with $\vec{E}||\hat{c}$

where the effect of the dipole matrix elements is dominant. The joint density of states at 3.0eV in $\vec{E}\perp\hat{c}$ are the same as in $\vec{E}||\hat{c}$. Similar to the 2.2eV structure, the dipole moments are weaker in the case of $\vec{E}\perp\hat{c}$. The slightly higher reflectivity at 3.3eV compared to the structure at 3.0eV in both theory and experiment is due to additional contributions of 35→39 in the region near XY plane and 35→40 transitions near Γ. The overall ratio of the calculated reflectivities for the two polarizations in considering transitions of 4 valence bands to 4 conduction bands is about 1.4. From the above indentifications for various structure in the spectra, we therefore believe that the large optical anisotropy of SbSI is mainly due to the difference in the dipole matrix elements for the two polarizations.

Comparing the two sets of the calculated reflectivities, the ones involving less bands give the ratio 1.17 and 2.06 for two polarizations at 2.3 and 3.0eV respectively, whereas, the dashed curves in Fig. 3 give the ratio of 1.2 at 2.2eV. The peak at 3.0eV is smeared out for the reflectivity including more bands with $\vec{E}\perp\hat{c}$. The general shape of the reflectivities with transitions of 4 valence bands to 4 conduction bands for $\hbar\omega\leq 3.0$eV and the ratio at 3.0eV agree better with the experimental data. However, the magnitudes of these reflectivities are smaller than the measured ones for $\hbar\omega\leq 3.5$eV. This shows that the transitions involving other bands are important and necessary to give a better agreement between theory and experiment. Improvement on the present calculation can be achieved by adjusting the pseudopotential form factors, in particular, those of Sb. We plan to do it when the ultraviolet spectra of SbSI become available.

In conclusion, we should emphasize the preliminary nature of our calculations. The reasonable agreement between theory and experiment for $\hbar\omega \leq 3.0$eV,

obtained with no adjustment of the form factors is remarkable. This indicates that the method of scaling the atomic form factors in the calculations can be applied to very anisotropic crystals. This method is comparatively simpler than other methods for crystals with many atoms per unit cell. It is especially useful to understand the main features near the absorption edge in the optical spectra of more complex semiconductors.

** Research sponsered in part by the U.S. Atomic Energy Commission.

† Supported by the Air Force Office of Scientific Research, Air Force System Command, USAF, under Grant No. AFOSR-72-2353.

* On leave from Université de Paris, Paris VI, France.

†† Guggenheim Fellow, on leave at Laboratoire d' Optique Quantique, Orsay, France.

References

1. For example, A. Kirkuchi, Y. Oka and E. Sawaguchi, J. Phys. Soc. Japan, 23, 337 (1967).
2. For example, D. M. Bercha, V. Yu Slivka, N. N. Syrbu, I. D. Turganitsa and D. V. Chepur, Fiz. Tverd, Tela, 13, 276 (1971) (Trans. Sov. Phys. - Solid State, 13, 217 (1971)).
3. D. Berlincourt, H. Jaffe, W. Merz and R. Nitsche, Appl. Phys. Letters, 4, 61 (1964).
4. H. G. Häffle, H. Wachernig, C. Irslinger, R. Grisar and R. Nitsche, Phys. Stat. Sol. 42, 531 (1970).
5. Y. Yamada and H. Chihara, J. Phys. Soc. Japan, 21, 2085 (1966);

A. G. Khasabov and I. Ya Nikiforov, Izv. Akad. Nauk. SSR. Ser. Fiz. 34, 2480 (1970) (Trans. Bull. Acad. Sci. USSR, Phys. Ser. 34, 2204 (1970)).

6. Y. R. Shen, "Proc. of International Conf. on Moldulation Spectroscopy", Tuscon, Arizona (Nov. 23-26, 1972) (to be published in Surface Sciences); R.R.L. Zucca, Ph.D. thesis (University of California, Berkeley, 1971) (unpublished).

7. M. L. Cohen and V. Heine, Solid State Phys. 24, 37 (1970).

8. J. P. Walter and M. L. Cohen, Phys. Rev. 183, 763 (1969).

9. C. Y. Fong and M. L. Cohen, Phys. Rev. Letters 21, 22 (1968).

10. Y. W. Tung and M. L. Cohen, Phys. Rev. 180, 823 (1969).

11. E. Dönges, Z. Anorg, Chem. 263, 112 (1950); R. W. G. Wyckoff, Crystal Structure, Vol. 1, 2nd ed., Interscience, p.385 (1963).

12. M. L. Cohen and T. K. Bergstresser, Phys. Rev. 141, 789 (1966).

13. D. Brust, Phys. Rev. 134, A 1337 (1964).

14. J. C. Slater, Quantum Theory of Molecules and Solids, Vol. 2, McGraw-Hill, p. 438 (1965).

15. G. Harbeke, J. Phys. Chem. Solids 24, 957 (1963).

Figure Captions

Fig. 1 Measured reflectivities and wavelength modulated spectra of SbSI. Arrows on the curves indicate the axes of scale.

Fig. 2 Band Structure of SbSI.

Fig. 3 Comparison between the experimental and calculated reflectivities.

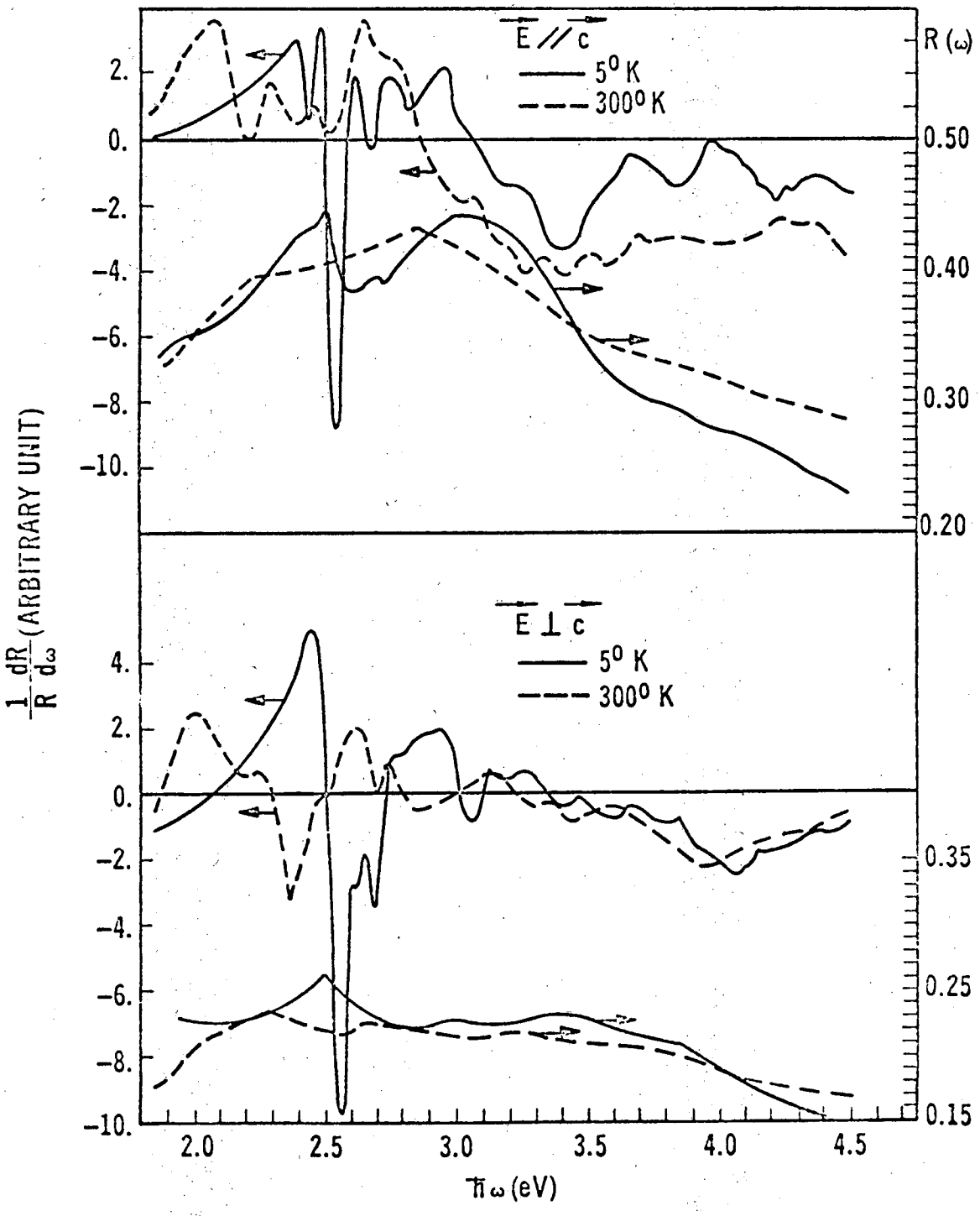
E // c
5° K
300° K
E ⊥ c
5° K
300° K
R (ω)
0.50
0.40
0.30
0.20
0.35
0.25
0.15
2.
0.
-2.
-4.
-6.
-8.
-10.
4.
2.
0.
-2.
-4.
-6.
-8.
-10.
2.0
2.5
3.0
3.5
4.0
4.5
ħω (eV)
$\frac{1}{R}\frac{dR}{d\omega}$ (ARBITRARY UNIT)

Fig. 1

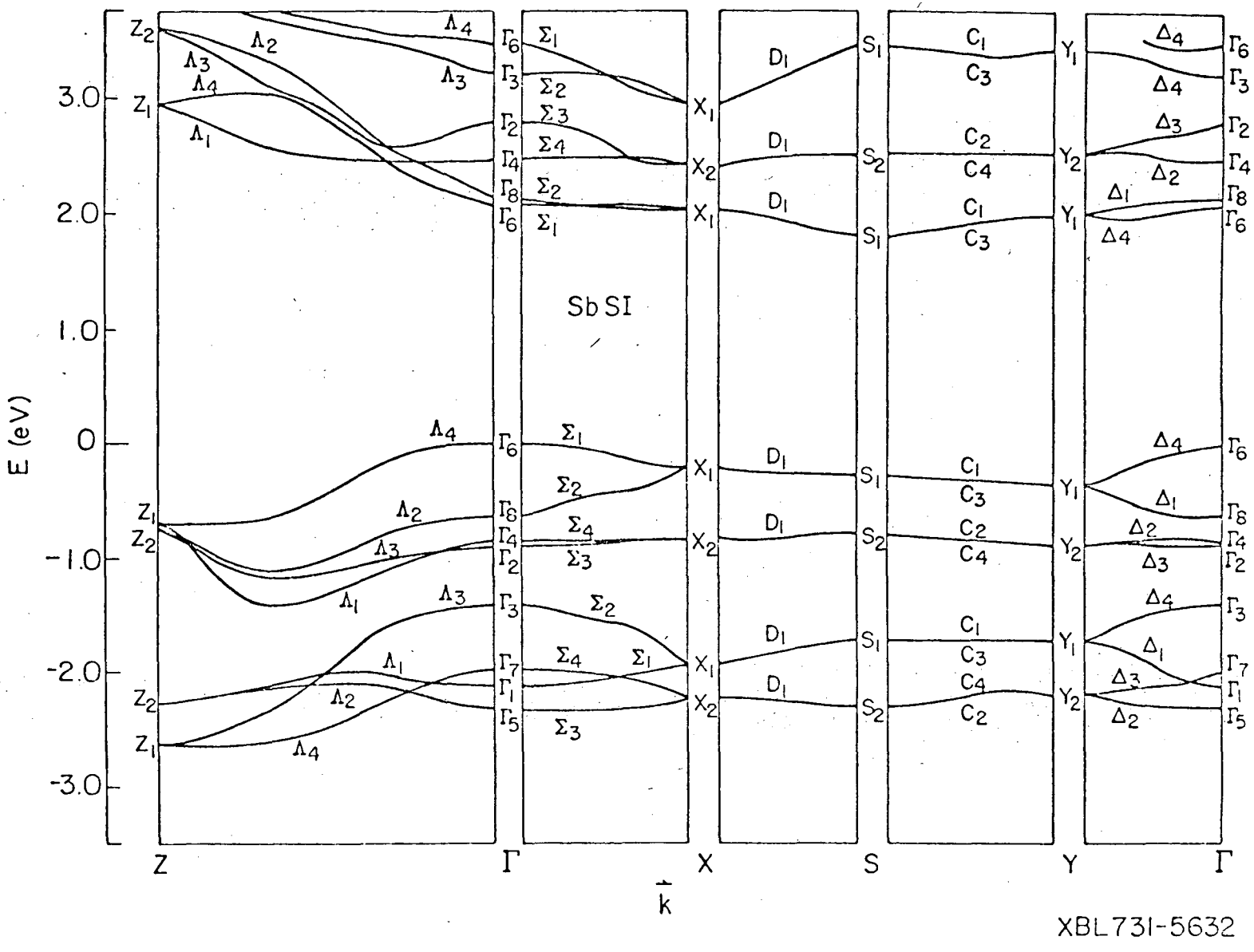

Fig. 2

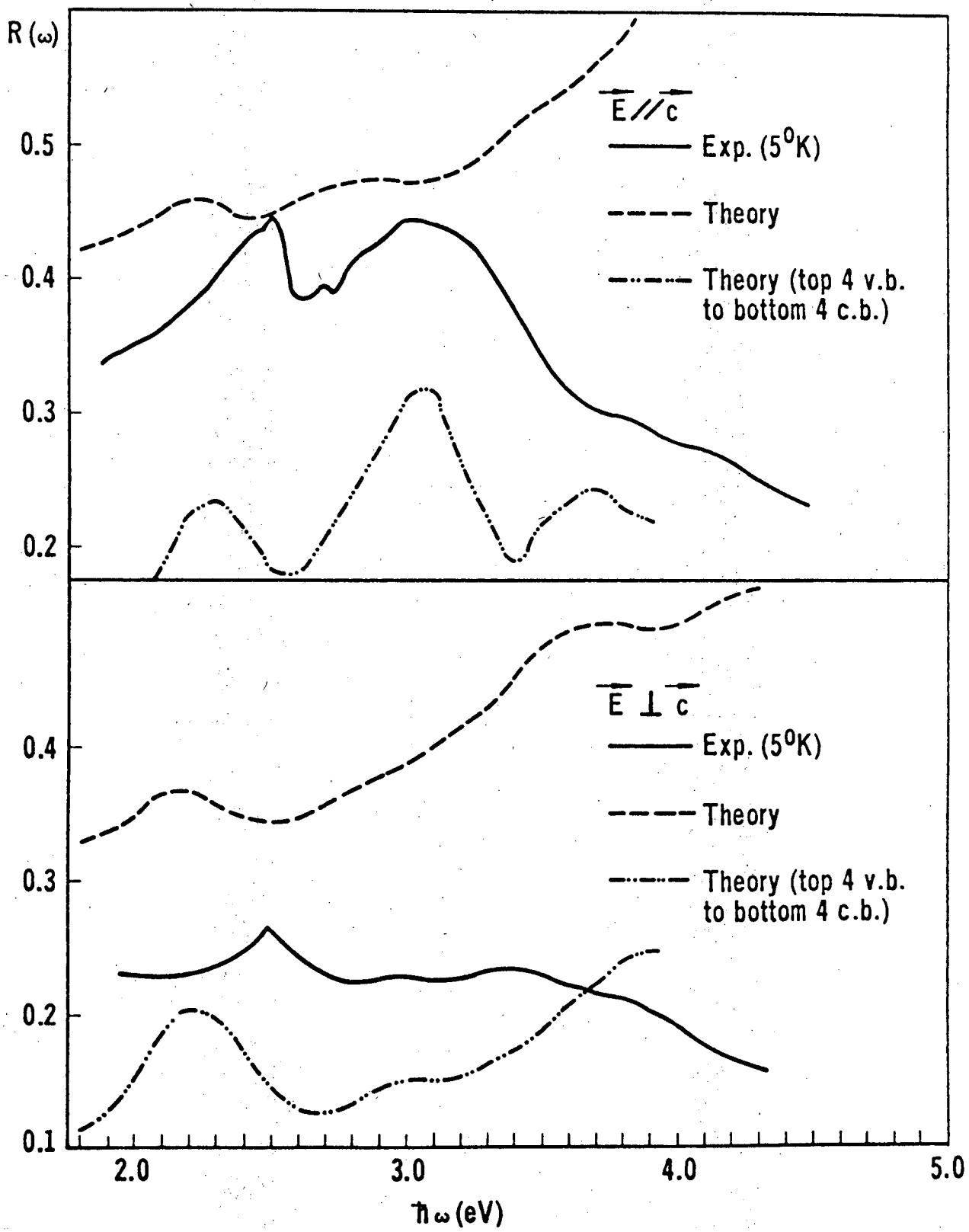
R (ω)
0.5
0.4
0.3
0.2
E // c
Exp. (5°K)
Theory
Theory (top 4 v.b. to bottom 4 c.b.)
0.4
0.3
0.2
0.1
E ⊥ c
Exp. (5°K)
Theory
Theory (top 4 v.b. to bottom 4 c.b.)
2.0
3.0
4.0
5.0
ħω (eV)

Fig. 3

TECHNICAL INFORMATION DIVISION
LAWRENCE BERKELEY LABORATORY
UNIVERSITY OF CALIFORNIA
BERKELEY, CALIFORNIA 94720